Chin. J. Astron. Astrophys. Vol. 6 (2006), No. 2, 165–174
(*http://www.chjaa.org*)

Chinese Journal of
Astronomy and
Astrophysics

Comptonization and Reprocessing Processes in Accretion Disks: Applications to the Seyfert 1 Galaxies NGC 5548 and NGC 4051 *

Fan Zhang and Xue-Bing Wu

Department of Astronomy, Peking University, Beijing 100871; *wuxb@bac.pku.edu.cn*

Received 2005 July 22; accepted 2005 October 11

Abstract Simultaneous multi-wavelength observations have revealed complex variability in AGNs. To explain the variability we considered a theoretical model consisting of an inner hot comptonizing corona and an outer thin accretion disk, with interactions between the two components in the form of comptonization and reprocessing. We found that the variability of AGNs is strongly affected by the parameters of the model, namely, the truncated disk radius $r_{\rm min}$, the corona radius r_s, the temperature KT_e and the optical depth τ_0 of the corona. We applied this model to the two best observed Seyfert 1 galaxies, NGC 5548 and NGC 4051. Our model can reproduce satisfactory the observed SEDs. Our fits indicate that NGC 5548 may have experienced dramatic changes in physical parameters between 1989–1990 and 1998, and that NGC 4051 has a much larger truncated disk radius (700 Schwarzschild radii) than NGC 5548 (several tens of Schwarzschild radii). Since we adopted a more refined treatment of the comptonization process rather than simply assuming a cut-off power law, our results should be more reasonable than the previous ones.

Key words: accretion – accretion disks – galaxies: active – galaxies: individual (NGC 5548, NGC 4051) – galaxies: Seyfert – X-rays: galaxies

1 INTRODUCTION

To explain the observed spectral energy distribution (SED) of AGNs in the optical/UV/X-ray bands, we usually need to use a two-component model consisting of a blackbody component and a power-law-like one. There is general consensus that the thermal emission comes from an optically thick accretion disk. However, for the power-law-like X-ray spectrum, various theories have been proposed. Among them, one suggests that the X-ray radiations are from magnetic reconnection (Di Matteo 1998; Galeev, Posner & Vaiana 1979; Haardt & Maraschi 1991; Di Matteo, Celotti & Fabian 1997; Di Matteo, Celotti & Fabian 1999), while another suggests that a hot, comptonizing corona produces the X-ray spectrum (Sunyaev & Titarchuk 1980; Sunyaev & Titarchuk 1985; Titarchuk 1994; Hua & Titarchuk 1995). Two key elements in the latter theory are the comptonization and reprocessing (Chiang & Blaes 2001, 2003). These two processes occur between the centrally located comptonizing region of plasma and the outer encircling thin accretion disk. Thermal emissions from the disk enter the plasma and provide seed photons for the comptonization process, and X-ray radiations from the plasma in turn illuminate the outer disk where high-energy photons are

* Supported by the National Natural Science Foundation of China.

reprocessed into UV/optical radiation. The reprocessed X-ray flux adds to the flux produced by viscous dissipation within the disk, producing the total thermal emission from the surface of the accretion disk. Therefore, these two processes reflect a physical link between the outer disk and the inner corona. Furthermore, this model suggests a possible way of explaining the correlated flux variations of the optical/UV and X-ray continua. However, more detailed discussions are needed to explain the full complexity of the observations.

Previous observations found no simple correlation between the X-ray and UV/optical continuum variations in some Seyfert galaxies (see Uttley 2005 for a review). Here we just mention a few examples. During April 13–16, 1998, HST observations were taken of NGC 3516 for 10.3 hours at UV wavelengths and for 2.8 days at optical wavelengths, simultaneously monitored by the RXTE (Rossi X-ray Timing Explorer) and ASCA (Advanced Satellite for Cosmology & Astrophysics) at the same time period (Edelson et al. 2000). The optical continuum bands showed small variations, while the flux in the shorter UV bands were almost constant. Lack of correlation between the optical and X-ray variations showed that the reprocessing region must be larger than 1 light-day in size, but simultaneous variations in the optical bands implied that the size of the reprocessing region should be smaller than 0.3 light-day (Edelson et al. 2000). These observations argue against a simple reprocessing model because of the contradictory conclusions.

For NGC 7469, it does not show any obvious correlation between the UV and 2–10 keV X-ray flux variations, but does show a correlation between the UV flux variations and the changes in the X-ray spectral slope (Nandra et al. 2000; Petrucci et al. 2004). This phenomenon is considerably less common in Seyfert galaxies, where a strong correlation between the spectral slope and the 2–10 keV flux is usually observed (Markowitz, Edelson & Vaughan 2003).

In addition, Done et al. (1990) found that there is no obvious optical variations in NGC 4051 during a 3-day observation, while at the same time strong X-ray variations were seen. Edelson et al. (2000) also showed that there is no obvious relationship between the variations in optical/UV and X-ray bands on timescales of a day or less in NGC 4051. The same thing also happens in Akn 564, another narrow line Seyfert 1 galaxy, which showed strong X-ray variability but weak optical flux variations (Shemmer et al. 2001).

However, NGC 5548, for which the best long-term simultaneous optical and X-ray light curves have been obtained, shows a tight correlation between the optical and X-ray variation with comparable amplitudes on longer time-scales of years (Uttley et al. 2003). If the optical variations are the result of the X-ray variability, as predicted by the reprocessing model, the amplitude of X-ray variations should be larger than the optical, which seems to be contrary to the observations. Though the existence of reprocessing process in NGC 5548 can not be rejected by the observations completely, it appears that these phenomena are difficult to be explained in a simple way.

In this paper, we propose an improved model which involves both comptonization and reprocessing processes to explain the simultaneous observed optical, UV, and X-ray data of NGC 5548 and NGC 4051. Because we adopted a more refined treatment of comptonization process rather than assuming a simple cut-off power law (Chiang & Blaes 2001, 2003), the derived parameters in our model from fitting the observed data seem more reasonable than those in previous works. Moreover, with our model we can give reasonable explanations of the observed SEDs and variability properties of these AGNs (as reviewed by Uttley 2005), which proved to be too complicated to be explained by the previous models.

In Section 2, we introduce our semi-analytic calculations of the spectral energy distributions of AGNs based on the improved two-component model. In Section 3, we describe the optical, UV and X-ray data of NGC 5548 and NGC 4051, and present our fitting results and explanations of the complex variability of the AGNs. Finally, a discussion and conclusions are given in Section 4.

2 TWO-COMPONENT MODEL AND SEMI-ANALYTIC CALCULATIONS

We consider a two-component model (see Fig. 1). One component is an outer thin accretion disk, another is a centrally located, spherical region consisting of hot plasma (usually named "corona"). The disk is truncated by the corona of radius r_s at an inner radius $r_{\rm min}(r_s > r_{\rm min})$, so some of soft photons produced by local viscous dissipation in the disk within the corona can enter the corona and be comptonized, which results in higher energy photons. As a consequence, the temperature

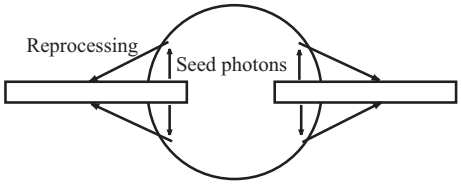

Fig. 1 Schematic diagram of the two-component model: the centrally located spherical corona, and the outer, thin disk truncated at an inner radius $r_{\rm min}$. Some of the soft photons from the disk enter the corona and are comptonized, and in turn, the high energy photons from the corona illuminate the outer disk and are reprocessed.

KT_e of the corona decreases. In turn, the higher energy photons from the spherical corona may illuminate the outer thin disk and be reprocessed into thermal UV/optical radiation, so finally the total thermal emission exceeds the initial emission produced only by the local viscous dissipation within the disk. Through adjusting the parameters of the model we can obtain different spectral energy distributions in the X-ray, optical, and UV bands.

When the reprocessing of X-ray photons is not considered, the thermal emission in the disk is only from the viscous dissipation, then we have the equation (Shakura & Sunyaev 1973),

$$F_{\rm visc} = \frac{3}{8\pi}\frac{GM\dot{M}}{r^3}\Big[1-\Big(\frac{r_I}{r}\Big)^{\frac{1}{2}}\Big], \tag{1}$$

where M and $\dot{M}$ are the central black hole mass and accretion rate, r_I is the innermost stable circular orbit and usually taken to be $6{\rm GM}/c^2$ for a Schwarzschild black hole.

The emission produced in the disk by the reprocessing of incident X-ray photons can be expressed as

$$F_{\rm inc} = \frac{3}{16\pi^2}\frac{L_{\rm x}}{r_s^2}h\Big(\frac{r}{r_s}\Big), \tag{2}$$

where $L_{\rm x}$ is the X-ray luminosity of the comptonizing plasma, and $h(\frac{r}{r_s})$ is an auxiliary function given by Zdziarski, Lubinski & Smith (1999, see also Chiang 2002). For $r > r_s$, the expression of $h(\frac{r}{r_s})$ can be simplified

$$h\Big(\frac{r}{r_s}\Big) \approx \frac{\pi}{4}\Big(\frac{r}{r_s}\Big)^{-3}. \tag{3}$$

So, the total thermal emission from the disk is

$$F_{\rm disk} = F_{\rm visc} + (1-A)F_{\rm inc}\,, \tag{4}$$

where A is the disk albedo.

Under normal conditions, $r \gg r_I$, the expression above can be further simplified into

$$F_{\rm disk} = \frac{1}{r^3}\Big[\frac{3}{8\pi}GM\ \dot{M} + (1-A)\frac{3}{64\pi}L_{\rm x}r_s\Big]. \tag{5}$$

When the disk emission seen by an observer at a luminosity distance d_l at an inclination angle i, the observed flux F_v is given by

$$F_v = \frac{4\pi\cos i}{d_l^2}\frac{hv^3}{c^2}\int_{r_s}^{\infty}\frac{rdr}{f_{\rm col}^4[\exp(hv/k_BT_{\rm disk}f_{\rm col})-1]}\,, \tag{6}$$

where $T_{\rm disk}$ is the effective temperature of the outer disk and $f_{\rm col}$ is a temperature-dependent color correction factor (Shimura & Takahara 1995). We assume a Hubble parameter H_0 of 67 km s^{-1} Mpc^{-1} in this paper.

The generalized Comptonization model describes in detail the theory of the X-ray spectrum that arises from the plasma. Titarchuk (1994, hereafter T94) showed that the X-ray spectrum is related to the distribution of the number of scattering, μ, the photon undergoes before escaping. Photons that suffer much fewer scatterings than average retain their initial information, and only photons who have undergone many more scatterings than average will affect the X-ray spectrum. Based on the theory that the X-ray spectrum is produced by hot electrons upscattered by low-frequency photons, the X-ray spectrum can be obtained by solving the Comptonization Stationary Equation

$$L_\nu N_1 - \beta N_1 = -\psi(x). \tag{7}$$

Here $L_\nu = \frac{\Theta\lambda_{tr}^{-1}(x\Theta)}{x^2}\frac{\partial}{\partial x}[\eta(x\Theta,\Theta)(\frac{\partial}{\partial x}+E)]$, N_1 is the occupation number, $\psi(x)$ is the initial spectrum of source photons emitted from the truncated disk within the corona and β has the expression,

$$\beta = \frac{\pi^2}{3(\tau_0+2/3)^2}\Big(1 - e^{-0.7\tau_0} + e^{-1.4\tau_0}\ln\frac{4}{3\tau_0}\Big), \tag{8}$$

where $x = h\nu/kT_e$ is the dimensionless photon energy, $\Theta = kT/m_ec^2$ is the dimensionless plasma temperature and τ_0 is the optical depth.

In the optically thick case ($\tau_0 \gg 1$), the spectrum of photons emerging from the corona can be simplified to the following equations (T94):

$$F_\nu(x,x_0) = \frac{\alpha_0(\alpha_0+3)}{2\alpha_0+3}\frac{1}{x_0}\Big(\frac{x}{x_0}\Big)^{3+\alpha_0}, \qquad \text{when} \quad 0 \le x \le x_0, \tag{9}$$

and

$$F_\nu(x,x_0) = \alpha_0(\alpha_0+3)\frac{e^{-x}}{x_0}\Big(\frac{x}{x_0}\Big)^{-\alpha_0}\frac{\int_0^\infty t^{\alpha-1}(x+t)^{\alpha+3}e^{-t}dt}{\Gamma(2\alpha+4)} \qquad \text{when} \quad x \ge x_0\,. \tag{10}$$

Here $\Gamma(x)$ is the Γ function, and $\alpha(x)=\sqrt{9/4+\gamma(x)}-3/2$, $\alpha_0=\sqrt{9/4+\gamma_0}-3/2$, while $\gamma=\frac{\beta\lambda_{tr}}{\Theta\mu}$, $\gamma_0=\frac{\beta}{\Theta[1+f_0(\Theta)]}$, $\mu=\eta(x\Theta,\Theta)/z^4$, and $\eta(z,\Theta)=\frac{z^4}{1+4.6z+1.1z^2}[1+\frac{f_0(\Theta)}{1+10.2z}]$, $f_0(\Theta) = 2.5\Theta+1.875(\Theta)^2(1-\Theta)$, where $z = h\nu/m_ec^2$, $\lambda_{tr}(z) = [1+2.8(1-1.1\Theta)z-0.44z^2]$.

In the optically thin case ($\tau_0 \ll 1$), γ and γ_0 in the above expressions will be replaced by (T94),

$$\gamma = \gamma_0(1+4.6z+1.1z^2) \quad \text{and} \quad \gamma_0 = \frac{\beta[1+(15/8)\Theta]}{\Theta[1+(19/8)\Theta]}\,. \tag{11}$$

The frequency-dependent disk albedo can be expressed as

$$1 - A_\nu = \sqrt{\frac{\pi}{3}\frac{h\nu}{m_ec^2}}\,. \tag{12}$$

Therefore, we can obtain the expression of $(1-A)$ in Eq. (4) as

$$1 - A = 1 - \frac{\int_0^\infty A_\nu F_\nu d\nu}{\int_0^\infty F_\nu d\nu} = \sqrt{\frac{\pi}{3}\frac{kT_e}{m_ec^2}}\frac{\Gamma(3/2-\alpha)\Gamma(\alpha+4.5)}{\Gamma(3/2)\Gamma(\alpha+4)\Gamma(1-\alpha)}\,. \tag{13}$$

3 APPLICATIONS TO NGC 5548 AND NGC 4051

3.1 Data of NGC 5548 and NGC 4051

Now we apply the above model to the two well-observed Seyfert 1 Galaxies, NGC 5548 and NGC 4051. For NGC 5548, we take $M = 1.0\times10^7\,M_\odot$, $\dot{M} = 0.02\,M_\odot\mathrm{yr}^{-1}$, and the inclination angle to be 45°. These values are not in conflict with the reverberation mapping estimates (Kaspi et al. 2000). Similarly, for NGC 4051, we take $M = 1.0\times10^6\,M_\odot$, $\dot{M} = 0.05\,M_\odot\ \mathrm{yr}^{-1}$, and

Table 1 Optical, UV and X-ray continuum parameters for the period 1980–1990 Ground-based/IUE/Ginga data of NGC 5548

Epoch	JD–2,440,000	$F^{a}_{5100\mathring{A}}$	$F^{a}_{2670\mathring{A}}$	$F^{a}_{1840\mathring{A}}$	$F^{a}_{1350\mathring{A}}$	$F^{b}_{2-10\,\mathrm{keV}}$	Γ
1	7535–7539	0.78 ± 0.08	2.22 ± 0.19	4.52 ± 0.22	7.45 ± 0.33	3.39	1.56 ± 0.19
2	7556	0.62 ± 0.06	2.09 ± 0.20	3.91 ± 0.22	6.18 ± 0.33	5.43	1.72 ± 0.03
3	7685	0.67 ± 0.06	1.72 ± 0.23	2.88 ± 0.31	3.94 ± 0.46	4.71	1.71 ± 0.10
4	8036–8037	0.50 ± 0.06	1.31 ± 0.36	2.56 ± 0.30	3.84 ± 0.35	3.87	1.68 ± 0.06
5	8039–8041	0.51 ± 0.07	1.44 ± 0.25	2.85 ± 0.36	4.25 ± 0.42	3.53	1.78 ± 0.06
6	8047	0.49 ± 0.07	1.40 ± 0.19	2.59 ± 0.30	4.21 ± 0.35	2.94	1.75 ± 0.08
7	8056	0.50 ± 0.06	1.53 ± 0.17	2.80 ± 0.21	4.35 ± 0.24	4.95	1.74 ± 0.04
8	8068	0.39 ± 0.05	1.10 ± 0.13	1.64 ± 0.30	2.23 ± 0.35	2.44	1.53 ± 0.04
9	8077	0.34 ± 0.05	0.96 ± 0.20	1.30 ± 0.30	1.74 ± 0.35	1.93	1.71 ± 0.14

[a] In units of 10^{-14} erg cm^{-2} s^{-1} Å^{-1}; [b] In units of 10^{-11} erg cm^{-2} s^{-1}. The IUE, optical and Ginga data were taken from Clave et al. (1991, 1992), Peterson et al. (1991) and Magdziarz et al. (1998), respectively.

Table 2 Optical continuum fluxes and X-ray continuum parameters from the 1998 Ground-based/RXTE data of NGC 5548

Epoch	JD–2,440,000	$F^{a}_{5100\mathring{A}}$	$F^{b}_{2-10\,\mathrm{keV}}$	Γ
1	979.96–980.40	1.16 ± 0.06	8.0	1.86 ± 0.03
2.1	985.09–985.40	1.17 ± 0.09	7.8	1.86 ± 0.03
2.2	985.69–986.41	1.18 ± 0.09	9.8	1.93 ± 0.02
2.3	986.65–987.40	1.16 ± 0.09	9.5	$1.90^{0.02}_{-0.01}$
2.4	987.63–987.86	1.24 ± 0.09	9.1	$1.91^{+0.04}_{-0.03}$
3.1	994.36–994.89	1.03 ± 0.04	6.9	$1.80^{0.05}_{-0.04}$
3.2	995.64–996.13	1.01 ± 0.08	5.6	$1.80^{0.03}_{-0.02}$

[a] In units of 10^{-14} erg cm^{-2} s^{-1} Å^{-1}; [b] In units of 10^{-11} erg cm^{-2} s^{-1}. The data are taken from Chiang et al. (2000).

Table 3 A summary of the optical continuum fluxes and X-ray continuum parameters of NGC 4051 in the years 1996 to 1998

Subset	Mean Flux[a] X-ray (2–10 keV)	Mean Flux[a] Continuum (5100Å)
Year 1	7.87 ± 3.25	13.66 ± 0.82
Year 2	6.42 ± 4.95	12.16 ± 0.76
Year 3	1.97 ± 1.81	12.06 ± 0.69

[a] X-ray flux in 2–10 keV band in counts s^{-1}, continuum flux in units of 10^{-15} erg cm^{-2} s^{-1} Å^{-1}. The data are taken from Peterson et al. (2000).

$\cos i = 0.96$. The values of the inclinations for NGC 5548 and NGC 4051 adopted here are also consistent with the values obtained by Wu & Han (2001).

Table 1 lists the data from simultaneous ground-based/IUE/Ginga observations of NGC 5548 from 1989 January to 1990 July. The IUE data were described in Clave et al. (1991, 1992), and the optical fluxes at 5100Å were obtained from ground-based observations by Peterson et al. (1991). The Ginga data were reported by Nandra et al. (1991) and re-extracted by Magdziarz et al. (1998).

Table 2 lists the data from the simultaneous EUVE, ASCA, and Ginga observations of NGC 5548 in the period 1998 June to August. The observations were described in Chiang et al. (2000).

Table 3 gives a summary of the optical and X-ray continuum fluxes of NGC 4051 in the period 1996 January to 1998 July, described in Peterson et al. (2000).

3.2 Previous Results on NGC 5548

In a previous work Chiang & Blaes (2003) considered the reprocessing process and explained the X-ray radiations resulting from hot electrons upscattered by low frequency photons. They modeled the X-ray spectrum simply with an exponentially cutoff power law , $L_E \propto E^{1-\Gamma}\exp(-E/E_c)$, where $E_c = 2k_BT_e$. Their model parameters fitted to the 1980–1990 Ground-based/IUE/Ginga data of NGC 5548 are summarized in the left part of Table 4.

Table 4 Model parameters fitted to the 1989–1990 Ground-based/IUE/Ginga data of NGC 5548

	Results of Chiang & Blaes (2003)					Our results				
Epoch	$r_{\rm min}^{\rm a}$	$T_0^{\rm b}$	$r_s^{\rm a}$	$k_BT_e^{\rm c}$	τ	$r_{\rm min}^{\rm a}$	$k_BT_e^{\rm c}$	$r_s^{\rm a}$	τ	A
1	2.20	4.0	2.07	683	0.13	2.18	96	1.99	1.52	0.32
2	1.85	4.2	2.07	153	0.72	1.89	103	2.10	1.10	0.16
3	3.36	2.8	3.70	66	1.64	2.60	85	2.77	1.56	0.24
4	2.31	3.3	2.42	76	1.54	2.38	86	2.42	1.36	0.23
5	2.07	3.6	2.47	96	1.05	2.21	76	2.35	1.39	0.29
6	1.97	3.7	2.22	226	0.44	1.97	70	2.29	1.60	0.32
7	1.96	3.7	2.19	37	2.46	2.18	78	2.28	1.78	0.28
8	2.57	2.8	2.17	85	1.82	2.03	75	1.98	1.96	0.24
9	2.62	2.7	2.76	50	2.05	2.05	52	2.12	2.10	0.40

[a,b,c] In units of 10^{14} cm, 10^4 K and keV, respectively.

From Table 4 it can be found that at epoch 1, Chiang & Blaes (2003) indicated that the comptonizing photons temperature gets to 683 keV, which seems to be unusually high. At such a high temperature, electrons will produce electron-positron pairs. Then the comptonizing process will probably be affected, and it is difficult to be sure whether or not the comptonizing process takes place. Taking an overall view of the whole data, we find that in the successive observations, the comptonizing photon temperature shows sharp jumps, while the photon flux changes little. Chiang & Blaes (2003) did not give a reasonable explanation of this phenomenon.

In another popular work (Titarchuk 1994), the generalized comptonizing model was discussed, but the work did not consider the reprocessing process.

3.3 Results on NGC 5548 and NGC 4051

Using the two-component model described in Section 2, we can fit the observed SEDs of the AGNs with new parameters. We consider both the comptonization process described in the generalized comptonizing model (T94) (rather than taking a simple cut off power law as in Chiang & Blaes (2003)) and the reprocessing process. The main parameters in our model are: the truncated disk radius $r_{\rm min}$, the corona radius r_s, the temperature KT_e, the optical depth τ_0 of the corona, and the disk albedo. In comparison with the results of Chiang & Blaes (2003), the fitting parameters in our model change more smoothly and reasonably over the observational period (see the right part of Table 4). Also, the model can possibly be used to explain the correlation between the observations in different continuum bands. Figures 2 and 3 show the SEDs that have been fitted to the data of NGC 5548 observed during 1989–1990 and in 1998. Figure 4 shows the SEDs fitted to the data of NGC 4051 observed during 1996–1998. In Tables 4, 5 and 6 we list our adopted fitting parameters of NGC 5548 and NGC 4051. Our fits are reasonably good for both NGC 5548 and NGC 4051.

Our results indicate that NGC 5548 may have undergone dramatic changes in physics parameters between 1990 and 1998. For observations in 1989–1990, we have derived a truncated disk radius around 2×10^{14} cm (70 Schwarzschild radii), a corona temperature around 80 keV and an optical depth around 1.5. For 1998, the corresponding values we derived are around 5×10^{13} cm (17

Schwarzschild radii), around 130 keV and around 0.15. These are consistent with the observational fact that both the optical and X-ray flux are higher in 1998 than in 1990. For the 1996–1998 observations of NGC 4051, we derived a truncated disk radius around 2×10^{14} cm (700 Schwarzschild radii), a corona temperature around 130 keV and an optical depth around 1. It may be noted that there is a significant difference in the truncated disk radius between NGC 5548 and NGC 4051.

3.4 Explaining the Complex Variability of AGNs

We can use the disk plus corona model to explain the complex variability observed in AGNs. The predicted spectrum is affected by changing the model parameters. The truncated radius $r_{\min}$ is the main parameter of the outer disk, and the radius r_s and the temperature T_e of the inner corona are the primary parameters influencing the X-ray spectrum. Here we outline a simple explanation of the observed complex variability in terms of our model and leave detailed investigations for a future paper.

The phenomenon that, in some AGNs, variations in the X-ray are observed before variations in the optical band, can be explained by our model. Now, a change in the coronal parameters will

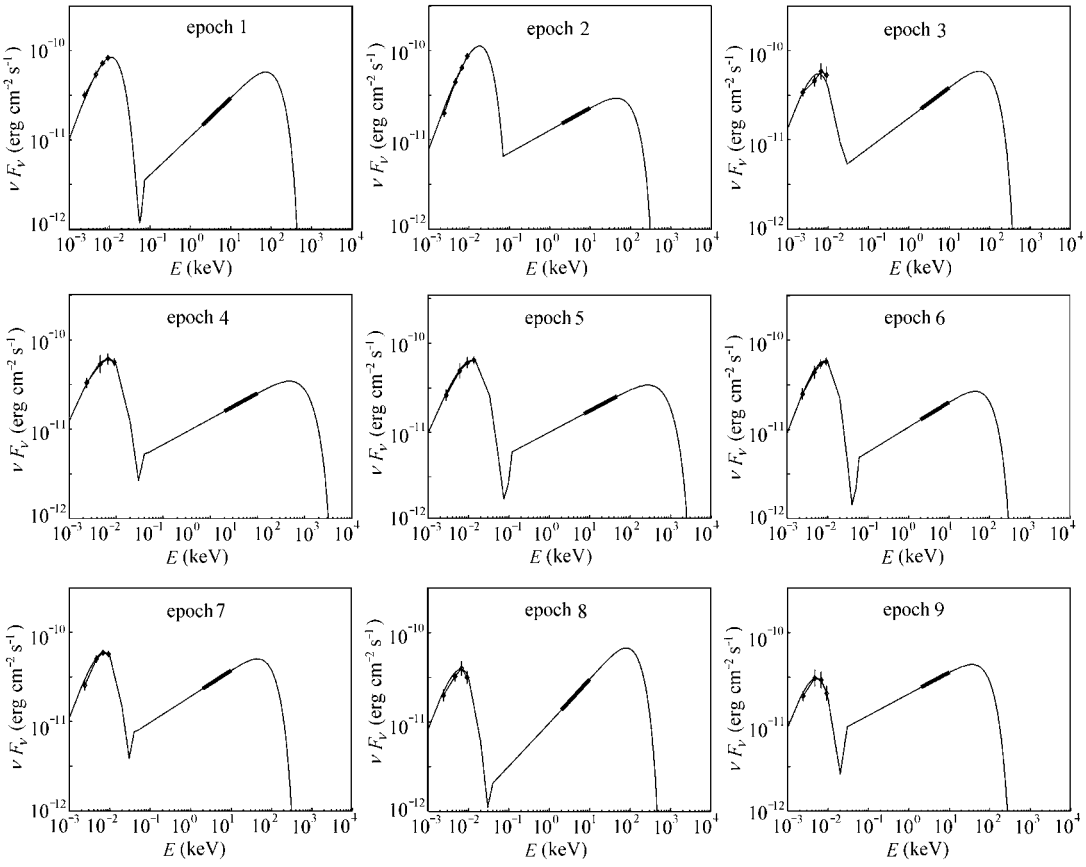

Fig. 2 SEDs fitted to the optical, UV and X-ray data of NGC 5548 at nine epochs in 1989–1990. The optical/UV data are plotted as diamonds and the power-law fit to the 2–10 keV Ginga data marked by thick line segments. These SEDs are obtained from our semi-analytic calculations described in Section 2.

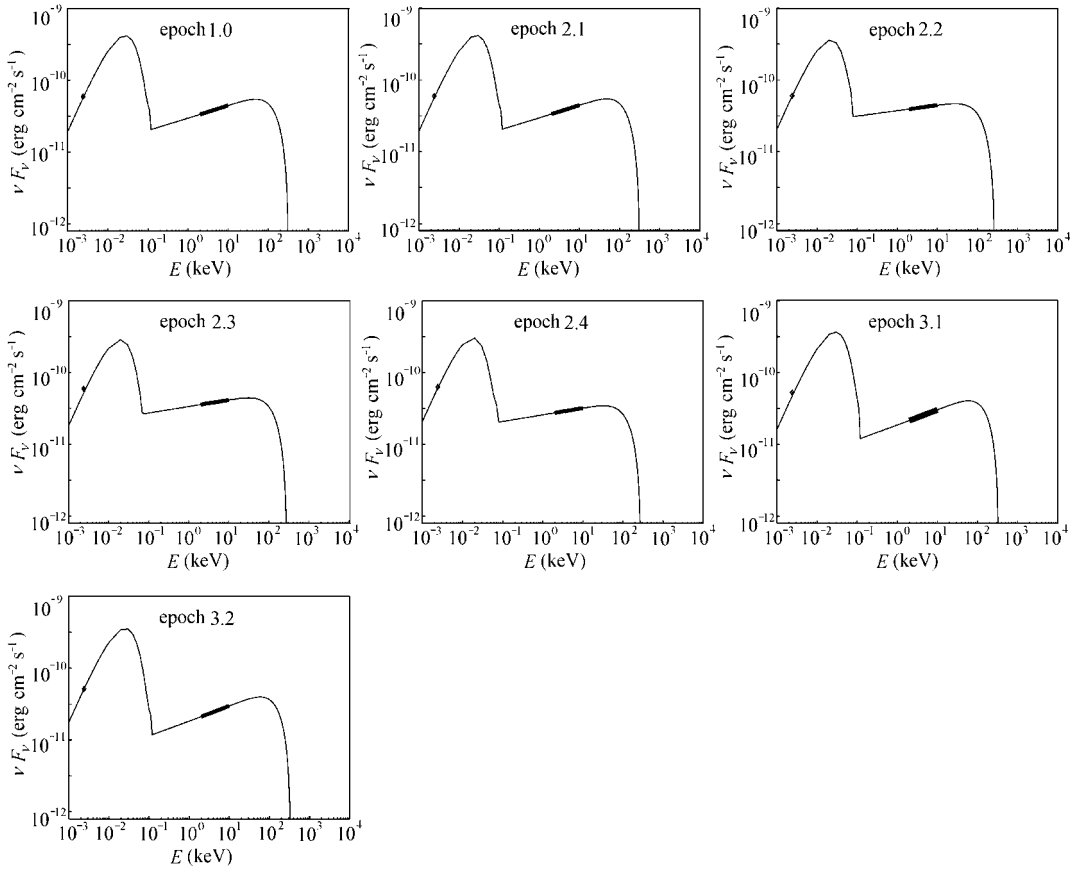

Fig. 3 SEDs fitted to the optical and X-ray data of NGC 5548 at seven epochs in 1998. The optical data are plotted as diamonds and the power-law fit to the 2–10 keV Ginga data marked with thick line segments.

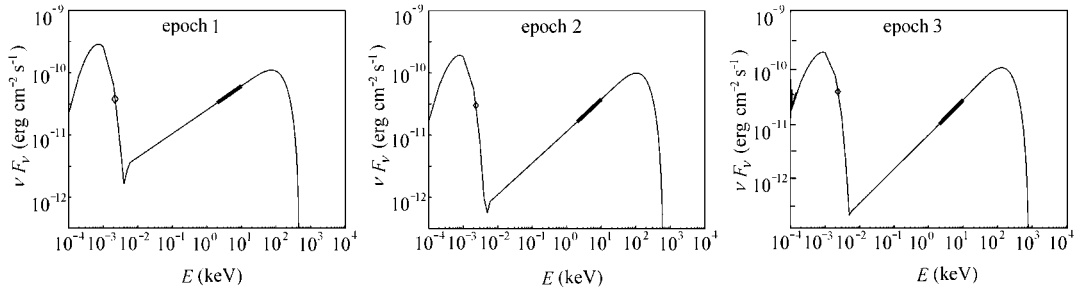

Fig. 4 SEDs fitted to the optical and X-ray data of NGC 4051 in the period 1996 January to 1996 July.

Table 5 Model parameters fitted to the 1998 Ground-based/RXTE data of NGC 5548

Epoch	$r_{\min}$ ($\times 10^{14}$ cm)	$k_B T_e$ (keV)	r_s ($\times 10^{14}$ cm)	τ	A
1	0.37	126	0.43	0.17	0.13
2.1	0.36	128	0.44	0.18	0.12
2.2	0.47	135	0.49	0.11	0.13
2.3	0.49	132	0.5	0.12	0.11
2.4	0.59	142	0.68	0.11	0.09
3.1	0.32	122	0.42	0.14	0.11
3.2	0.38	148	0.40	0.15	0.03

Table 6 Adopted model parameters to fit to the data of NGC 4051 of 1996–1998

Epoch	$r_{\min}$ ($\times 10^{14}$ cm)	$k_B T_e$ (keV)	r_s ($\times 10^{14}$ cm)	τ	A
1	2.73	137	2.93	0.85	0.10
2	1.98	141	1.05	2.10	0.08
3	1.63	122	1.72	1.49	0.18

result in a change in the X-ray flux, so if the reprocessing process is all-important, then variations in X-ray would cause variations in the optical, and the X-ray variations would precede the optical variations. In some AGNs, we have the opposite situation where the optical variation precedes the X-ray. This can also be explained by our model. For a change in the inner radius of the disk will result in a change of the optical flux, so if the comptonizing process is all-important then optical variability will drive X-ray variability and optical variation will precede X-ray variation.

The complexity of the interaction between the disk and the corona indicates that the two processes, reprocessing and comptonization, are in a state of rivalry. If these two rival processes are at equilibrium, changing either one will not account for the correlation between the UV/Optical and 2–10 keV X-ray flux variations. On the other hand, if the rivals are unequal in intensity (as in the cases considered), then there will be the observed complex correlation between the different bands.

4 CONCLUSIONS AND DISCUSSION

Our conclusions are summarized as follows:

(1) With our improved two component model, we can give a satisfactory explanation of the correlated flux variations of the optical/UV and X-ray continuum of NGC 5548 and NGC 4051. Because we adopted an explicitly model for X-ray radiation produced by Comptonization process rather than by simply assuming a cut-off power law as in some previous studies, our derived model parameters are more reasonable.

(2) Our results indicate that NGC 5548 may have experienced dramatic changes in its physics parameters between 1989–1990 and 1998. Specifically, the truncated disk radius may have changed from 70 to 17 Schwarzschild radii and the optical depth of the corona, from 1.5 to 0.15. We also found that there is a significant difference in the derived truncated disk radius (of about 700 Schwarzschild radii) between the broad line Seyfert 1 galaxy NGC 5548 and the narrow line Seyfert 1 galaxy NGC 4051, clearly reflecting a dramatic difference in accretion disk structure between these two sources.

(3) Observations found complex correlation between the X-ray and UV/optical continuum in many Seyfert galaxies, and our model can give a possible interpretation of this phenomenon. The complex variability may be explained in terms of different relative importance between comptonization and reprocessing in the accretion flow. The complex variability cannot easily be explained by any of the previous models because they do not involve both the reprocessing and Comptonization processes.

However, the two-component model we adopted in this paper is still very simple and more detailed works are needed to be done in the future. For example, we did not make a time-dependent check on the disk and corona structure, which should be considered when attempting to explain the variability of AGNs. Furthermore, the disk and corona structure may not remain the same if the accretion rate changes (Kong et al. 2004). Especially the inner hot corona may become ADAF (Advection-dominated Accretion Flow) if the accretion rate gets lower than a certain critical value (Narayan & Yi 1994), which could affect the predicted spectrum substantially. A future improved model can be expected to find application in other Seyfert galaxies.

Acknowledgements We thank Fukun Liu for helpful discussions. This work was partly supported by the NFSC Grants (Nos. 10473001 and 10525313), the RFDP Grant (No. 20050001026) and the Key Grant Project of Chinese Ministry of Education (No. 305001).

References

Chiang J., 2002, ApJ, 572, 79
Chiang J., Blaes O., 2001, ApJ, 557, L15
Chiang J., Blaes O., 2003, ApJ, 586,97
Chiang J., Reynolds C. S., Blaes O. et al., 2000, ApJ, 528,292
Clave J., Reichert G. A., Alloin D. et al., 1991,ApJ, 366, 64
Clave J., Nandra K., Makino F. et al., 1992, ApJ, 393, 113
Di Matteo T., 1998, MNRAS, 299, L15
Di Matteo T., Celotti A., Fabian A. C., 1997, MNRAS, 291, 805
Di Matteo T., Celotti A., Fabian A. C., 1999, MNRAS, 304, 809
Done C., Ward M. J., Fabian A. C. et al., 1990, MNRAS, 243, 713
Edelson R., Koratkar A., Nandra K. et al., 2000, ApJ, 534, 180
Galeev A. A., Rosner R., Vaiana G. S., 1979, ApJ, 229, 318
Haardt F., Maraschi L., 1991, ApJ, 380, L51
Hua X.-M., Titarchuk L., 1995, ApJ, 449, 188
Kaspi S., Smith P. S., Netzer H. et al., 2000, ApJ, 533, 631
Kong M. Z., Wu X. B., Han J. L. et al., 2004, ChJAA, 4, 518
Magdziarz P., Blaes O. M., Zdziarski A. A. et al., 1998, MNRAS, 301, 179
Markowitz A., Edelson R. Vaughan S., 2003, ApJ, 598, 935
Nandra K., LE T., George I. M. et al., 2000, ApJ, 544, 734
Nandra K., Pounds K. A., Stewart G. C. et al., 1991, MNRAS, 248, 760
Narayan R., Yi I., 1994, ApJ, 428, L13
Peterson B. M., Balonek T. J., Barker E. S. et al., 1991, ApJ, 368, 119
Peterson B. M., McHardy I. M., Wilkes B. J. et al., 2000, ApJ, 542, 161
Petrucci P. O., Maraschi L., Haardt F. et al., 2004, A&A, 413, 477
Shakura N. I., Sunyaev R. A., 1973, A&A, 24, 337
Shemmer O., Romano P., Bertram R. et al., 2001, ApJ, 561, 162
Shimura T., Takahara F., 1995, ApJ, 445, 780
Sunyaev R. A., Titarchuk L. G., 1980, A&A, 86, 121
Sunyaev R. A., Titarchuk L. G., 1985, A&A, 143, 374
Titarchuk L. G, 1994, ApJ, 434, 570 (T94)
Uttley P., 2005, invited review at conference on "AGN variability from X-ray to radio", Crimea, June 2004; to appear in ASP conference series (astro-ph/0501157)
Uttley P., Edelson R., McHardy I. M. et al., 2003, ApJ, 584, L53
Wu X.-B., Han J. L., 2001, ApJ, 561, L59
Zdziarski A. A., Lubinski P., Smith D. A., 1999, MNRAS, 303, L11